ACS APPLIED MATERIALS & INTERFACES

RESEARCH ARTICLE

www.acsami.org

Increasing the Thermal Storage Capacity of a Phase Change Material by Encapsulation: Preparation and Application in Natural Rubber

Songpon Phadungphatthanakoon,[†,‡] Sirilux Poompradub,[§] and Supason P. Wanichwecharungruang*[,†]

[†]Department of Chemistry, Faculty of Science, [‡]National Center of Petroleum, Petrochemicals and Advanced Materials, and [§]Department of Chemical Technology, Faculty of Science, Chulalongkorn University, Bangkok 10330, Thailand

ABSTRACT: Existing encapsulated organic phase change materials (PCM) usually contain a shell material that possesses a poor heat storage capacity and so results in a lowered latent heat storage density of the encapsulated PCM compared to unencapsulated PCM. Here, we demonstrate the use of a novel microencapsulation process to encapsulate n-eicosane (C20) into a 2:1 (w/w) ratio blend of ethyl cellulose (EC): methyl cellulose (MC) to give C20-loaded EC/MC microspheres with an increased heat storage capacity compared to the unencapsulated C20. Up to a 29 and 24% increase in the absolute enthalpy value during crystallization and melting were observed for the encap-C20/EC/MC microparticles with a 9% (w/w) EC/MC polymer content. The mechanism that leads to the increased latent heat storage capacity is discussed. The blending of the water-dispersible C20-loaded EC/MC microspheres into natural rubber latex showed excellent compatibility, and the obtained rubber composite showed not only an obvious thermoregulation property but also an improved mechanical property.

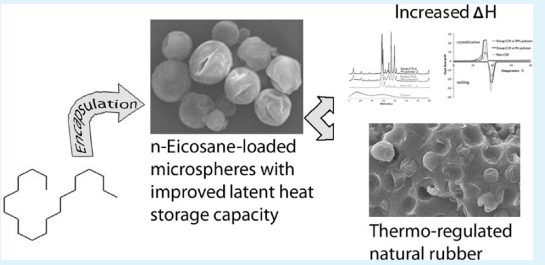

KEYWORDS: phase change material, microencapsulation, energy storage, crystallization, latent heat

INTRODUCTION

Phase change materials (PCM) are a form of latent heat storage system that have been demonstrated as an acceptable energy storage in various applications, such as thermoregulated building materials,[1,2] heat transfer media,[3,4] heat and solar energy storage devices,[5−7] and thermoregulated fabrics.[8,9] Paraffin and fatty acids possess a phase change temperature in the range of normal human environments and with an outstanding energy storage density. Thus, they are very popular for applications involving temperature regulation for human comfort, such as building materials, thermoregulated fabrics and furniture. Their problems, namely their leakage in the melted state, incompatibility with polar materials, chemical instability, and the associated large volume change upon the phase change, have been lessened by encapsulation into various shell materials. A few examples from among the vast number of shell materials used for the entrapment of paraffin and fatty acids include silica,[10,11] graphite,[4] polyurea,[12] gelatin/acacia,[13] melamine−formaldehyde,[14,15] urea−formaldehyde,[16,17] polymethylmethacrylate,[18,19] polyethylene glycol (PEG)−carbohydrates, such as PEG−cellulose, PEG−agarose, and PEG−chitosan,[20] acrylic-based polymers,[21] and diatomites.[22] At present, most research has used a loading ratio of approximately 3:1 (w/w) of PCM: shell material. Therefore, the shell material, which by itself possesses a poor heat storage capacity, takes up a large percentage (25% (w/w)) of the mass of the encapsulated PCM and so lowers the latent heat storage density of the whole material. Thus, a higher percentage of the encapsulated PCM is needed in the blend in order to achieve any given heat storage efficiency, and this increased loading level usually affects the mechanical property of the final composite. In addition to the encapsulation approach, the addition of polymeric materials or gelators into the PCM has also been used to solve the leakage problem.[23]

Here, in this work, we demonstrate the fabrication of n-eicosane (C20)-loaded microspheres through a simple yet novel process using a 2:1 (w/w) ratio blend of ethyl cellulose (EC):methyl cellulose (MC) as a shell material. More importantly, the process gave the C20-loaded EC/MC microspheres an increased latent heat storage density compared to the unencapsulated C20. The mechanism that induces the increased heat storage capacity is discussed. In addition, the application of the obtained PCM (encap-C20/EC/MC) microspheres into natural rubber (NR) latex to prepare thermoregulated NR with improved mechanical properties is also reported here for the first time.

EXPERIMENTAL SECTION

Chemicals. EC and MC were purchased from Sigma-Aldrich (St. Louis, Mo, USA). C20 (99%) was from Acros organics (Geel, Belgium). NR latex of 60% (w/v) dry rubber content (60 DRC) was from the Thai Rubber Latex Corporation, Bangkok, Thailand.

PCM Encapsulation. The microencapsulation of C20 was carried out by a novel liquid to solid encapsulation process using two weight ratios of C20 to polymer (EC and MC) of 4:1 and 10:1. To this end, EC (266 mg) was dissolved in 25 mL of ethanol and then the MC solution

Received: July 3, 2011
Accepted: September 1, 2011
Published: September 01, 2011

(133 mg of MC dissolved in 10 mL of water) was added and stirred until a clear transparent solution was obtained. Then, C20 (1.59 or 3.99 g) was added into the polymeric solution that was maintained at 60 °C followed by 80 mL of hot water (60 °C), which was slowly dropped into the mixture while being continuously homogenized at 6000 rpm. After that, the emulsion was cooled down to 0 °C while still homogenizing at the same speed for another 15 min. The obtained encapsulated C20 suspension was subjected to ethanol removal under vacuum and the aqueous suspension of PCM (encap-C20/EC/MC) microspheres was either freeze-dried or centrifuged (30,000 g; 5 min), with the floating pellet being harvested and dried under vacuum. The dry samples were subjected to analysis by scanning electron microscopy (SEM) on a JEM 6400 (JEOL, Tokyo, Japan), transmission electron microscopy (TEM) on a H-7650, 100 kV electron microscope (HITACHI, Japan), differential scanning calorimetry (DSC) at a heating and cooling rate of 10 °C/min under a nitrogen flow of 20 mL/min (METTLER, DSC 822, USA) and X-ray powder diffraction (XRD) on a Rigaku DMAX 2200/Ultima+ diffractometer (Rigaku International Corporation, Tokyo, Japan).

Loading Determination. Loading of the obtained PCM products (C20 loaded EC/MC particles) was determined from the ^{1}H NMR spectrum of the product. The product was dissolved in $CDCl_3$ and subjected to ^{1}H NMR analysis at 400 MHz (Varian Company, USA). The ratio of the EC/MC polymer to the C20 was then calculated from the ratio of the integration of resonance peaks representing the EC/MC polymer chains (δ of 3.0−4.4 ppm, H1−H6 and $-OCH_3$ and $-OCH_2-$ of the sugar backbone) and those for C20 (δ of 0.87 ppm, 6 H of the terminal $-CH_3$). The % loading is then derived as follows

$$\%\text{loading} = 100 \times \text{weight of C20 in product} / (\text{weight of polymer in product} + \text{weight of C20 in product})$$

Recycling Stability of the Microcapsules. The freeze-dried encap-C20/EC/MC was heated to 50 °C for 5 min and then cooled to 25 °C for 5 min. This process was repeated for 200 heating−cooling cycles (25−50−25 °C) and the material was then evaluated for any changes in the microparticle size and morphology by SEM, heat storage capacity by DSC, and water dispersion ability by dispersing the material in distilled water.

Thermoregulated NR. Thermoregulated NR was prepared by mixing the water suspension of the encap-C20/EC/MC microparticles with NR latex. The 60 DRC NR latex (12.5 g, containing 7.5 g dry rubber mass) was mixed with water slurry of encap-C20/EC/MC (10 mL, containing 6.0 g of C20 and 1.5 g of the EC/MC polymer) by stirring for 20 min. The obtained mixture was then poured into a 14 × 14 × 0.2 cm mold and air-dried at 25 °C. The dry PCM-rubber piece was then subjected to tensile strength analysis with a Universal Testing Machine (LR 10K PLUS, England). In addition, the PCM-rubber was subjected to heat treatment at 100 °C in an oven for 20 min.

Thermoregulation of the PCM-rubber was tested using cut out circles, each of 5.2 cm diameter and 0.315 cm thickness. The room temperature (28 °C) control and PCM-rubber (no encap-C20/EC/MC microspheres added and with 50% (w/w) encap-C20/EC/MC microspheres, respectively) pieces were put onto a temperature-controlled surface at 50−52 °C and the images were recorded by thermal camera (ISI, Infrared Solutions SnapShot, USA) at various times. In a reverse manner, the rubber pieces preheated to 46 °C were left to cool on a room temperature (28 °C) surface and the images were recorded in the same manner.

RESULTS AND DISCUSSION

Encapsulation. C20 encapsulation into a EC/MC polymeric shell (encap-C20/EC/MC) was successfully prepared through a novel liquid to solid encapsulation process using EC with 33.3% (w/w) MC as the shell material. The 2:1 (w/w) ratio of EC:MC was found to be the optimal ratio of the polymer mixture for obtaining the highest C20 loading (data not shown), and so this ratio was used throughout this study. The process involved slowly adding warm water into a warm ethanolic solution of the C20 PCM and EC/MC polymer mix under a homogenizing condition, then solidifying the formed microspheres by lowering the temperature of the system to 4 °C (lower than the melting temperature of the C20). Ethanol was evaporated from the obtained white slurry and the slurry was dried by either freeze-drying or by harvesting by centrifugation and low-pressure evaporation of the pellet. Here, we demonstrate the preparation of encap-C20-EC/MC microparticles at two C20: polymer weight ratios of 4:1 and 10:1, which corresponded to encap-C20/EC/MC products composed of 20 and 9% (w/w) of EC/MC polymer material, respectively, and with C20 loadings of 80 and 91% by weight in the final dry product, respectively. SEM and TEM analyses of the two different resultant products showed a core−shell microspherical architecture (Figure 1) with diameters of 4.73 ± 0.62 and 5.92 ± 1.15 μm for the particles with 20% and 9% (w/w) polymer, respectively. DLS analysis gave broadly agreeable hydrated particle sizes of 7.69 ± 5.95 and 6.78 ± 2.90 μm for the 20 and 9% (w/w) polymer microparticles, respectively. Freeze-drying and low-pressure vacuum drying gave similar sized and morphology encap-C20/EC/MC spheres, as observed by SEM and TEM (data not shown). In addition, complete water dispersibility of the encap-C20/EC/MC particles was obtained, which indicated that all the water immiscible hydrophobic C20 molecules were encapsulated into the microspheres. Indentation of the microparticles was very obvious for all the dry particles in the TEM and SEM images (Figure 1), and is likely to be a result of some volume changes upon the solidification of the C20 during the microsphere preparation process.

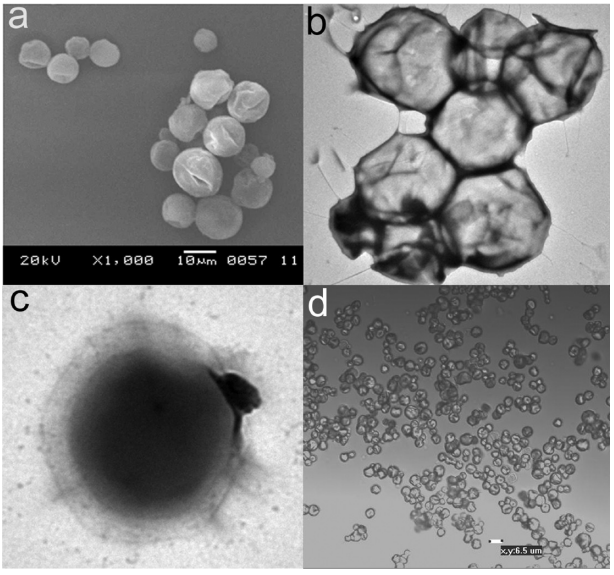

Figure 1. Representative (a) SEM, (b, c) TEM, and (d) optical microscopic images of the encap-C20/EC/MC particles prepared with a 9% (w/w) polymer content.

The encapsulation mechanism is unknown for certain but we speculate that one possibility is as follows. At 60 °C in the ethanolic solution of the polymers, the C20 molecules, which are not soluble in ethanol, were homogenized into microdroplets

Scheme 1. N-Eicosane (C20) Encapsulation[a]

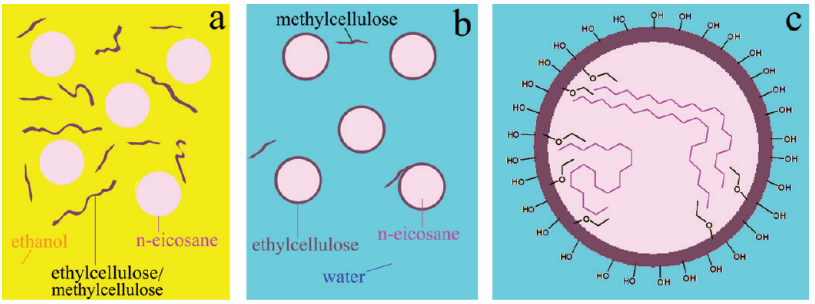

[a] (a) Under homogenization at 60 °C, droplets of C20 were suspended in the ethanolic solution of ethylcellulose (EC) and methylcellulose (MC). (b) With a slow change from ethanol to water, the EC polymer chains arrange themselves around the C20 droplets forming the water dispersible C20-encapsulated spheres. (c) The arrangement of the self-assembled spheres is such that the surface of the particle is covered with hydroxyl moieties of the EC polymer chains and the hydrophobic ethoxy groups of the polymer are in contact with the C20 molecules inside the sphere. Not shown is the entrapping some MC within the EC shell structures.

suspended in the solution. Then upon the slow addition of a large amount of water into the system, the EC chains, which are not soluble in water, arranged themselves around the C20 droplets in such a way that the hydrophilic hydroxyl groups had maximum contact with water molecules while the hydrophobic ethoxyl groups had minimum contact with water and maximum contact with the C20 molecules. This proposed self-assembling of the polymer chains around the microdroplets makes the obtained polymeric wrapped microdroplets dispersible in water without the need of any additional surfactant molecules, even after the stopping of the homogenization (Scheme 1).

The proposed significant interaction between the hydrophobic ethoxy groups of the EC chains and the C20 molecules also likely affects the melting enthalpy of the C20 as discussed below in the Phase Transition section. During the self-assembling of the EC around the C20 droplets, the MC chains (present at 33% of the total polymer mass) are likely to be trapped and entangled into the polymeric shell of the microspheres. The presence of the MC chains at the polymeric wall of the microspheres helps the spheres to be more stably dispersible in water. This assembling of the EC polymer chains into water dispersible microspheres instead of a water insoluble precipitate is possible due to the slow change of the medium from an ethanol-rich to a water-rich one, thus allowing enough time for the molecular arrangement of the polymer chains at the surface of the C20 microdroplets. The obtained water suspension of the microspheres was then cooled down to below the melting point of the C20, thus solidifying all the C20 inside the polymeric wall. The solidification of the core material automatically decreased its volume, thus accounting for the observed dents in the microspheres (Figure 1). The indentation of the wall of the microspheres correlates well with the maximum interaction between C20 molecules and the ethoxy moieties of the EC polymer chains and the thinness of the shell for the two ratios of polymer to C20 used (1:10 and 1:4).

It should be noted here that when the encapsulation was carried out at higher C20 to polymer ratios than 1:10 (w/w), in addition to the obtained product there was residual oily unencapsulated C20 in the suspension (data not shown). Products obtained from the encapsulation process at C20 to polymer ratios of 1:10 and 1:4 correspond to the calculated C20 loading of 91 and 80% (w/w), assuming 100% encapsulation efficiency. ^{1}H NMR analysis of the two products (using integration of resonance peaks from cellulose backbone at 3.0−4.4 ppm and that

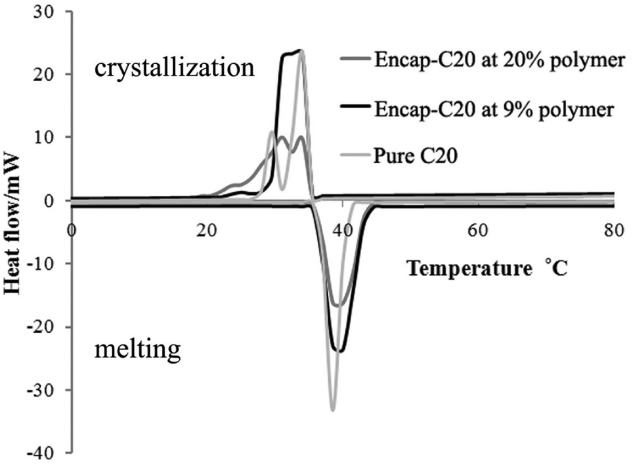

Figure 2. Representative DSC curves of unencapsulated C20 (pure C20) and encap-C20/EC/MC microparticles prepared with 9 and 20% (w/w) EC/MC polymer contents.

from the two terminal methyl groups of C20 at 0.87 ppm) gave the expected C20 loading levels of ∼80−90% and ∼70−80% (by weight), for the products prepared at C20:polymer ratios of 10:1 and 4:1, respectively. Therefore, it can be concluded that the encapsulation process was efficient and could be used to prepare encapsulated C20 spheres with up to 90% (w/w) loading capacity.

Phase Transition. Cooling down the unencapsulated C20 (pure C20) led to a first transition into the rotator phase at 34.2 °C and a second transition at 30.6 °C into the stable triclinic crystal phase[24] (Figure 2). The absolute enthalpy of the transition into the rotator phase during the cooling down was $50.5 \pm 4.0\ J\ g^{-1}$, whereas that of the second transition was $135.6 \pm 6.1\ J\ g^{-1}$. The heating showed only a single phase transition at 38 °C with an enthalpy value of $202.4 \pm 6.0\ J\ g^{-1}$, which was somewhat higher than the total absolute enthalpy value of the two-step crystallization ($186.1\ J\ g^{-1}$).

The freezing range (20−35 °C) and the melting range (35−45 °C) of the two encap-C20s were wider than that of the pure C20 (Figure 2), which indicates the likely interaction between the EC/MC polymer chains and the C20 molecules. Cooling down the encap-C20 led to multiple but overlapping transitions at 20−35 °C with total absolute enthalpy values for the encap-C20 prepared at a polymer weight contents of 20 and

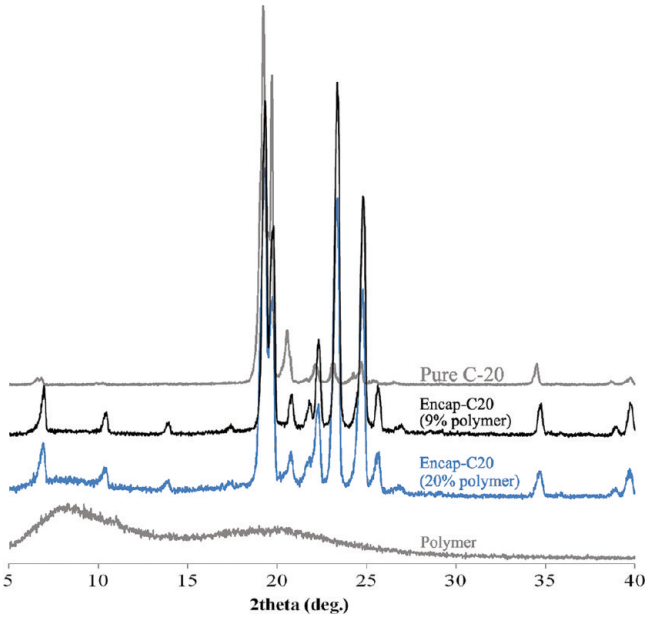

Figure 3. Representative XRD patterns of the unencapsulated C20 (pure C20), the polymer (2:1 (w/w) ratio EC: =MC blend), and the two encap-C20/EC/MC samples.

9% (w/w) of 204.5 ± 8.5 and 239.8 ± 3.8 J g^{-1}, respectively, a 10 and 29% increase compared to the pure C20 (186.1 J g^{-1}). The increase in the absolute enthalpy value during the phase transition of the encap-C20 was also observed for the heating process. As the temperature of the system increased, the bulk C20 showed a single phase transition with an enthalpy value of 202.4 ± 7.3 J g^{-1}, whereas the encap-C20 prepared at 20 and 9% (w/w) polymer contents also showed a single transition phase but with enthalpy values of 208.2 ± 9.4 and 251.4 ± 6.2 J g^{-1}, representing a 3 and 24% increase in the energy storage capacity, respectively.

The increase in the absolute enthalpy value during the crystallization of the two encap-C20/EC/MC products, compared to the pure C20, implied that the C20 molecules encapsulated in the EC/MC-based microparticles released more energy upon solidification. The DSC curve of the encap-C20 crystallization shows more multiplicities than that of pure C20, indicating that the C20 molecules inside the spheres undergo more phase transitions upon crystallization than the two distinct phase transitions of the pure C20. This multiple phase transition pathway leads to a higher energy release and results in a C20 crystal structure which is different from that of the pure C20, as indicated by their XRD patterns (Figure 3). Peaks at 2θ of 6.74, 10.36, 13.6, 17.04, 20.5, 34.42, and 39.62 are obvious in the XRD pattern of the encap-C20 but are very small or almost undetectable in that of the pure C20. The difference in the crystallinity of the encap-C20 and pure C20 also results in the observed differences in the melting enthalpy. In conclusion, our speculation is that the interaction of C20 and the EC/MC polymeric wall material interferes with the solidification of C20 inside the spheres in such a way that the transition is multistepped and more exothermic than that of the pure C20. The melting of the crystalline C20 inside the spheres was also more endothermic compared to that for the pure C20.

It is obvious that the encap-C20/EC/MC with 9% (w/w) polymer content shows a better energy storage capacity than does the one with 20% (w/w) polymer content. The explanation for this is that the contribution of the 11% increase in the polymer mass, which never melts at the tested temperature range, negatively compensates for the increase in the absolute enthalpy of the system. Although the DSC crystallization curve of the encap-C20/EC/MC with 20% (v/v) polymer content is broader than that with 9% (v/v) polymer content, they show a similar pattern regarding the number of phase transitions. Both DSC curves showed two major overlapped transitions at ∼34 and ∼32 °C with an approximately equal enthalpy contribution from the two. The situation for pure C20 is totally different, since the two transitions observed are of unequal contribution at 34.2 and 30.6 °C, with the major contribution to the total enthalpy value coming from the first transition (at 34.2 °C).

In summary, the increase in the absolute enthalpy value during the melting and crystallization of the encap-C20 in the EC/MC microspheres indicated that the material possessed a higher latent heat storage capacity than the unencapsulated C20. With the presence of 20 or 9% (w/w) of the EC/MC polymer, the materials showed a 3 and 24% increase in the ability to absorb heat, respectively, and a 10 and 29% increase in the ability to release thermal energy, respectively. As described earlier, the interaction between C20 and the EC/MC polymer is likely to play an important role in this phenomenon and so this situation will not occur with every pair of polymer/PCM materials. An encapsulation process that allows for a good specific interaction between the right polymers and the right PCM is also crucial. It should be mentioned here that all the previously reported microencapsulated C20 preparations showed at least a 30% decrease in the heat storage capacity (enthalpy of the phase transition) at a presence of 20% (w/w) polymer material.[25−27] This is the first report that showed an increase in the enthalpy value when the C20 was encapsulated into polymeric microspheres.

Stability of the Encap-C20/EC/MC Microparticles. Repeated heating and cooling of the encap-C20/EC/MC particles between 50 to 25 °C for 200 cycles (25−50−25 °C is one cycle), did not alter the appearance of the encap-C20/EC/MC particles prepared with a 20% (w/w) EC/MC polymer content. The treated material still showed good water dispersibility, which indicated no leakage of the hydrophobic C20 from the microspheres. In contrast, the encap-C20 prepared at 9% (w/w) polymer content showed leakage of the C20, i.e., the treated material did not disperse well in water and the undispersed material showed some waxy appearance. Thus, the polymeric wall of the 20% (w/w) EC/MC polymer particles is presumed to be thick enough to prevent the leaking of the encapsulated C20.

Natural Rubber with Thermoregulation Property. The water suspension of the encap-C20/EC/MC microspheres with a 20% (w/w) EC/MC polymer content could easily be mixed with the 60 DRC NR latex to obtain an encap-C20/EC/MC content of 50% (w/w), as calculated using the weight of dry encap-C20/EC/MC and dry rubber mass. A higher percentage of PCM microspheres in the rubber, e.g., 70% (w/w), resulted in rubber piece being easily cracked. At lower PCM microsphere contents, such as at 20% (w/w), the obtained milky white liquid could easily be poured into a mold, and the dry PCM-rubber piece showed good homogeneity when observed by eye. In addition, the SEM images of the PCM-rubber clearly indicated an excellent dispersion of the encap-C20/EC/MC microspheres in the rubber matrix (Figure 4 top). The PCM-rubber possessed an increased tensile (mechanical) strength with the compensation of a reduced elongation property (Figure 4 bottom), compared to the control rubber. The stress−strain curves of the PCM-rubber and control rubber revealed similar modulus values (stress values

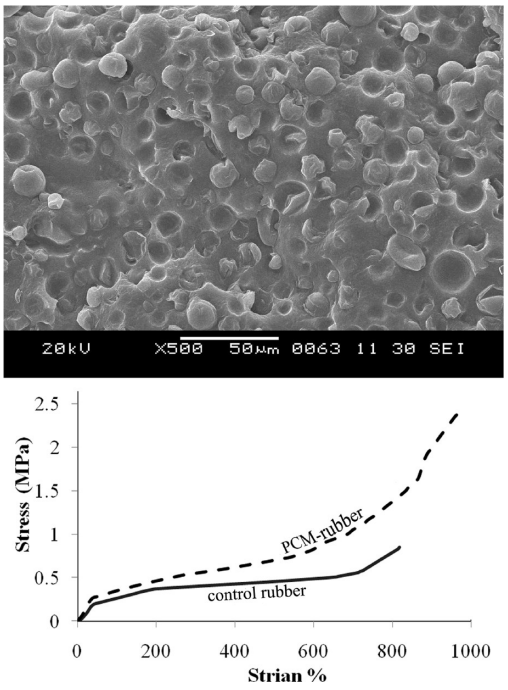

Figure 4. Top: Representative SEM image of the PCM-rubber. Bottom: Tensile stress−strain curve of the PCM-rubber derived with (PCM-rubber) or without (control rubber) the inclusion of 50% (w/w) encap-C20/EC/MC particles of a 9% (w/w) MC/EC polymer content.

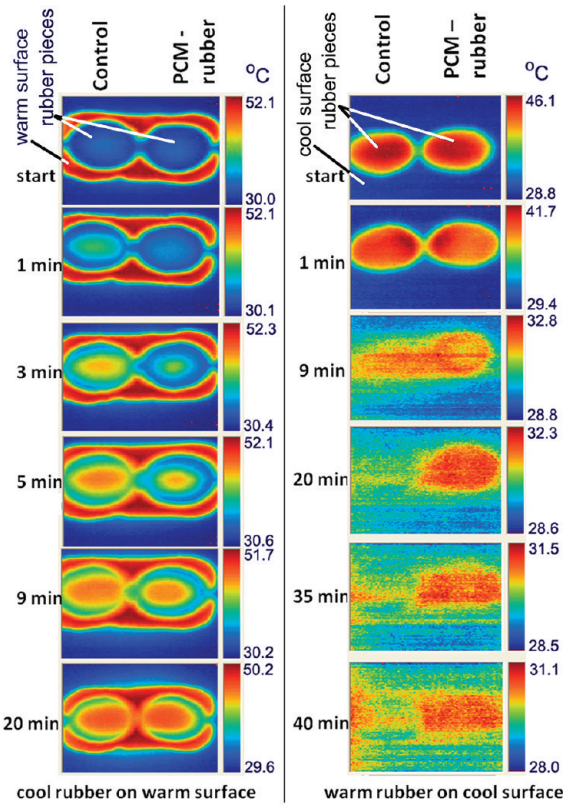

Figure 5. Representative thermal images showing the thermo-regulation property of the control and PCM-rubber. Left: The 28 °C control and PCM-rubber at various time points after putting onto a 50 °C surface. Right: The 46 °C control and PCM-rubber at various time points after putting onto a 28 °C surface.

at a given strain) up to an applied strain of 50%, but thereafter at higher strains the PCM-rubber showed a higher stress value. Compared to the control, the hardness of the PCM-rubber increased. This means that the encap-C20/EC/MC microspheres are good fillers that improve the mechanical strength of the rubber. The unmodified rubber breaks at a strain of about 800%, whereas the PCM-rubber can hold up to about 1000%.

The PCM-rubber piece could be kept at 80 °C for 10 min without any evidence of C20 leaking out of the rubber piece, as evaluated by the absence of an oily liquid in the rubber piece. Thus, the 20% (w/w) EC/MC polymer encap-C20 based PCM-rubber can withstand the high temperature normally required in the process of rubber goods production. Although the EC/MC-polymeric shell is thin (only 20% polymer present in the spheres), good dispersion of the spheres in rubber latex allows an excellent formation of a rubber wall around each sphere, and the rubber wall then acts as the container for the encap-C20/EC/MC sphere (Figure 4 top). Thus, the thin (and possibly relatively fragile — see Figure 1) polymeric shell is not an issue as the solidified rubber wall around the microspheres provide an additional strength element.

The thermoregulation property of the PCM-rubber could be observed clearly through a thermal camera. Here the test was carried out on a circular rubber piece (5.2 cm radius and 0.315 cm thick, containing 7.2 g each of the rubber and the 9% (w/w) EC/MC polymer encap-C20 particles). When transferred from room temperature (28 °C) onto a heated surface at 50−52 °C, the PCM-rubber piece maintained a temperature of less than 40 °C for 20 min, compared to the control, which reached 50 °C within 9 min (Figure 5).

Similarly, when the PCM-rubber pieces at 46 °C were placed at 28 °C, the PCM-rubber piece could maintain a temperature of over 30 °C for more than 40 min while the control rubber piece dropped to 29 °C within 15 min (Figure 5). Thus, with a good distribution of the encap-C20/EC/MC microparticles in the rubber matrix, the PCM-rubber piece possessed a reasonable thermoregulation property.

CONCLUSION

Here we demonstrate a unique microencapsulation of C20 using a 2:1 (w/w) ratio EC:MC polymer mix to give encap-C20/EC/MC microspheres with an increased heat storage capacity compared to the capacity of the pure C20. A 29 and 24% increase in the absolute enthalpy value during crystallization and melting were observed for the encap-C20 with the 9% (w/w) polymer content over that for the unencapsulated C20. It is likely that the interaction between the EC/MC polymer mix and the C20 causes a different phase transition path for the encap-C20 compared to the free C20. The new path contains multiple broad overlapped transition steps, releases more energy than the two-step crystallization of the pure C20 does, and gives crystals with a different XRD pattern. The water dispersible encap-C20/EC/MC microspheres dispersed well in NR latex and produced a thermoregulating rubber with improved mechanical strength. The potential use of such thermoregulated NR materials is likely to benefit diverse applications, such as mattresses and other furniture, swim-wear, shoes, hats, and so on.

AUTHOR INFORMATION

Corresponding Author
*Tel: (662)2187634. Fax: (662)2541309. E-mail: psupason@chula.ac.th.

ACKNOWLEDGMENT

The authors thank the Department of Architecture, Faculty of Architecture, Chulalongkorn University, for the thermal camera and also thank the following funding sources: the Thailand Research Fund, the Special Task force for Activating Research fund from the centenary academic development project, Chulalongkorn University, and the Thai Government Stimulus Package 2 (TKK2555). The authors are also very grateful for the English corrections from Robert Butcher of the Publication Counseling Unit, Faculty of Science, Chulalongkorn University.

REFERENCES

(1) Borreguero, A. M.; Carmona, M.; Sanchez, M. L.; Valverde, J. L.; Rodriguez, J. F. *Appl. Therm. Eng.* **2010**, *30*, 1164.
(2) Castellón, C.; Medrano, M.; Roca, J.; Cabeza, L. F.; Navarro, M. E.; Fernández, A. I.; Lázaro, A.; Zalba, B. *Renew. Energy* **2010**, *35*, 2370.
(3) Fang, G.; Li, H.; Chen, Z.; Liu, X. *Energy* **2010**, *35*, 4622.
(4) Hong, Y.; Ding, S.; Wu, W.; Hu, J.; Voevodin, A. A.; Gschwender, L.; Snyder, E.; Chow, L.; Su, M. *ACS Appl. Mater. Interfaces* **2010**, *2*, 1685.
(5) Li, H.; Liu, X.; Fang, G. *Energy Buildings* **2010**, *42*, 1661.
(6) Sharma, A.; Chen, C. R.; Murty, V. V. S.; Shukla, A. *Renew. Sust. Energy Rev.* **2009**, *13*, 1599.
(7) Sharma, A.; Chen, C. R.; Vu Lan, N. *Renew. Sust. Energy Rev.* **2009**, *13*, 1185.
(8) Fallahi, E.; Barmar, M.; Kish, M. H. *Iran. Polym. J.* **2010**, *19*, 277.
(9) Salaün, F.; Devaux, E.; Bourbigot, S.; Rumeau, P. *Thermochim. Acta* **2010**, *506*, 82.
(10) Fang, G.; Chen, Z.; Li, H. *Chem. Eng. J.* **2010**, *163*, 154.
(11) Miao, C.; Lü, G.; Yao, Y.; Tang, G.; Weng, D.; Qiu, J.; Mizuno, M. *Chem. Lett.* **2007**, *36*, 494.
(12) Zou, G. L.; Lan, X. Z.; Tan, Z. C.; Sun, L. X.; Zhang, T. *Acta Phys. Chim. Sin.* **2004**, *20*, 90.
(13) Hawlader, M. N. A.; Uddin, M. S.; Khin, M. M. *Appl. Energy* **2003**, *74*, 195.
(14) Zhang, X. X.; Fan, Y. F.; Tao, X. M.; Yick, K. L. *Mater. Chem. Phys.* **2004**, *88*, 300.
(15) Zhang, X. X.; Tao, X. M.; Yick, K. L.; Fan, Y. F. *J. Appl. Polym. Sci.* **2005**, *97*, 390.
(16) Jin, Z.; Wang, Y.; Liu, J.; Yang, Z. *Polymer* **2008**, *49*, 2903.
(17) Tseng, Y. H.; Fang, M. H.; Tsai, P. S.; Yang, Y. M. *J. Microencapsul.* **2005**, *22*, 37.
(18) Alay, S.; Göde, F.; Alkan, C. *Fiber. Polym.* **2010**, *11*, 1089.
(19) Wang, Y.; Xia, T. D.; Feng, H. X.; Zhang, H. *Renew. Energy* **2011**, *36*, 1814.
(20) Entürk, S. B.; Kahraman, D.; Alkan, C.; Göke, I. *Carbohyd. Polym.* **2011**, *84*, 141.
(21) Sánchez-Silva, L.; Tsavalas, J.; Sundberg, D.; Sánchez, P.; Rodriguez, J. F. *Ind. Eng. Chem. Res.* **2010**, *49*, 12204.
(22) Li, M.; Wu, Z.; Kao, H. *Sol. Energy Mater. Sol. Cells* **2011**, *95*, 2412.
(23) Zhang, X.; Deng, P.; Feng, R.; Song, J. *Sol. Energy Mater. Sol. Cells* **2011**, *95*, 1213.
(24) Montenegro, R.; Landfester, K. *Langmuir* **2003**, *19*, 5996.
(25) Zhang, X. X.; Fan, Y. F.; Tao, X. M.; Yick, K. L. *Mater. Chem. Phys.* **2004**, *88*, 300.
(26) Alkan, C.; Sari, A.; Karaipekli, A. *Energy Convers. Manage.* **2011**, *52*, 687.
(27) Lan, X. Z.; Tan, Z. C.; Zou, G. L.; Sun, L. X.; Zhang, T. *Chin. J. Chem.* **2004**, *22*, 411.